A Simple Free Energy Model for Weakly Interacting Polymer Blends

Anne-Valerie G. Ruzette[†] and Anne M. Mayes*

Department of Materials Science and Engineering, Massachusetts Institute of Technology, 77 Massachusetts Ave., Cambridge, Massachusetts 02139

Received April 21, 2000; Revised Manuscript Received January 8, 2001

ABSTRACT: Given the intrinsic relation between phase behavior and performance in applications involving polymer mixtures, the thermodynamics of these systems has been the common focus of a wide body of experimental and theoretical studies. An elusive goal in this research field has been the ability to predict or simulate the degree of thermodynamic compatibility of two distinct homopolymers based on pure component properties alone. In an attempt to address this need, we present a simple model for the free energy of mixing of compressible polymer blends, based on a modification of the regular solution model. Its ability to qualitatively capture the phase behavior of weakly interacting polymer pairs using only the pure component properties of mass density, solubility parameter, and thermal expansion coefficient is demonstrated. To this end, a wide range of blend chemistries is considered, spanning purely dispersive polyolefin systems to those comprising more polar components, such as poly(methyl methacrylate), poly(ϵ-caprolactone), and polycarbonate. The thermodynamic and molecular origin of the observed phase behavior for each of the systems studied is also discussed.

Introduction

Control over bulk thermodynamics is a key to success in most applications involving multicomponent polymeric materials such as blends and block copolymers. Yet, despite the great attention this subject has received, the ability to predict the thermodynamics of a given homopolymer pair based on pure component properties only remains an unsolved problem in polymer science. Particularly disturbing is the lack of simple thermodynamic tools that can serve as accurate guides in the design of new functional multicomponent polymeric compositions and chemistries with tunable thermodynamic behavior. This is especially discouraging considering the remarkable progress recently made in the area of polymer synthetic chemistry, which has facilitated the preparation of new macromolecules of countless architectures or compositions.

Two major features distinguish the thermodynamics of polymer mixtures in comparison with their small molecule analogues. First, the dramatically reduced combinatorial entropy upon mixing two macromolecules together typically results in mutual immiscibility in the absence of favorable enthalpic interactions between the two unlike segments. Consequently, most polymer mixtures form homogeneous phases only at extremely high temperatures or upon the addition of a common solvent. Second, and perhaps more interestingly, while most small molecule mixtures and alloys undergo phase separation primarily upon cooling through an upper critical solution transition (UCST) (Figure 1a), macromolecular mixtures are known to also undergo, in some instances, phase separation upon heating through a lower critical solution transition (LCST) as shown in Figure 1b.[1,2] The experimental observation of this inverted coexistence curve is also a direct consequence of the reduced combinatorial entropy of mixing in polymer mixtures. Under these circumstances, additional entropic factors otherwise negligible and arising from differences in the pure component pressure−volume−temperature ($P-V-T$) properties govern the free energy of mixing at elevated temperature and destabilize the mixture. This has been shown by several authors using equation-of-state (EOS) theories[3−11] such as the Prigogine−Flory theory[3−5] and the Sanchez−Lacombe lattice fluid model.[6,12]

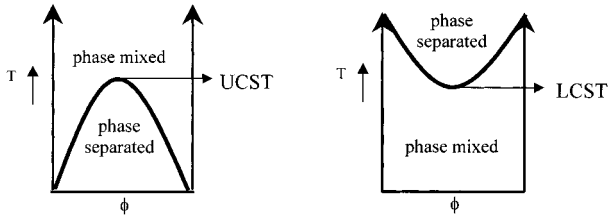

Figure 1. Schematic illustration of (a) UCST and (b) LCST-type phase diagrams.

The thermodynamics of polymer solutions and mixtures was first analyzed independently by Flory[13,14] and Huggins,[15,16] who derived, within a rigid lattice framework, the following regular solution model for the free energy of mixing per unit volume, Δg_{mix}, for two distinct homopolymers A and B or a polymer A and a solvent B ($N_B = 1$):

$$\Delta g_{mix}/kT = \frac{\phi_A}{N_A v_A} \ln \phi_A + \frac{\phi_B}{N_B v_B} \ln \phi_B + \frac{\phi_A \phi_B}{v} \chi^{FH} \quad (1)$$

where ϕ_i is the volume fraction and N_i the number of segments of volume v_i for molecules i, v is the average segmental volume $(v_A v_B)^{1/2}$, and χ^{FH} is the so-called Flory−Huggins interaction parameter. In eq 1, the first two terms represent the minute ($\sim 1/N_i$) entropy gain on mixing polymers A and B on the same lattice, while the last term represents the usually unfavorable enthalpic contribution to the free energy. The interaction

* To whom correspondence should be addressed.
[†] Current address: Elf-Atochem/CNRS, UMR 167, 95, Rue Danton, B. P. 108, 92303 Levallois-Perret, France.

10.1021/ma000712+ CCC: $20.00
Published on Web 02/15/2001

parameter χ^{FH} is related to the excess exchange interaction energy $\Delta\epsilon$ according to eq 2:

$$\chi^{FH} = z\left[\epsilon_{AB} - \frac{\epsilon_{AA} + \epsilon_{BB}}{2}\right]/kT = z\Delta\epsilon/kT \qquad (2)$$

where z is the lattice coordination number and ϵ_{ij} is the segmental attractive (<0) nearest-neighbor van der Waals interaction energy between segments i and j. The Flory−Huggins theory is a mean field formalism that assumes the system to be incompressible. It defines χ as being inversely proportional to temperature and independent of pressure, composition, molecular weight, and chain architecture. From the free energy expression given in eq 1, the well-known spinodal condition for phase separation in a symmetric blend ($\phi_A = \phi_B = 0.5$ and $\nu_A = \nu_B$) can be derived:

$$\chi_c^{FH} = \frac{1}{2}\left(\frac{1}{N_A^{1/2}} + \frac{1}{N_B^{1/2}}\right)^2 \qquad (3)$$

which reduces to $\chi_c^{FH}N = 2$ when $N_A = N_B = N$. Hence, according to the F−H incompressible regular solution model, the thermodynamics of the system at fixed N_i's is dictated by a single parameter: χ^{FH}, or, equivalently, $\Delta\epsilon$. Attempts have been made to predict this quantity from pure component properties only, without requiring the fitting of any blend-specific adjustable parameter from experimental data. To this end, the well-known Berthelot's mixing rule that assumes ϵ_{AB}, the cross-interaction energy, to be the geometric average of the pure component interaction energies ϵ_{AA} and ϵ_{BB}:

$$\epsilon_{AB} = \sqrt{\epsilon_{AA}\epsilon_{BB}} \qquad (4)$$

has typically been used.[17] The pure component interaction energy ϵ_{ii} is in turn related to the experimental Hildebrand solubility parameter δ, which is the square root of the cohesive energy density and has units of (energy$^{1/2}$/volume$^{1/2}$). According to the regular solution theory,[17] which further assumes an average segmental volume $v = \sqrt{v_A v_B}$ for the cross-interactions, χ^{FH} scales with the difference in individual component solubility parameters as

$$\chi^{FH} = \frac{v}{kT}(\delta_A - \delta_B)^2 \qquad (5)$$

Pure component solubility parameters can either be determined experimentally from homopolymer $P-V-T$ data[18] or calculated empirically using group contribution methods,[19] which evaluate homopolymer properties based on the contribution of each chemical group present in the repeat unit. When used in combination with the Hildebrand solubility parameter formalism, the Flory−Huggins regular solution model can thus serve to predict the degree of thermodynamic compatibility and phase behavior of weakly interacting polymer pairs from pure component properties. The underlying assumptions are **(**1**)** no volume changes on mixing, **(**2**)** ideal entropy of mixing, **(**3**)** weak forces of the induced dipole type (dispersive interactions), and **(**4**)** Berthelot's rule for the cross-interaction energy (eq 4). Such a formalism implies the interaction parameter χ^{FH}, purely enthalpic in nature, is always positive and monotonically decreases with increasing temperature (UCST-type phase behavior), and miscibility only occurs when the solubility parameters of the individual components are of similar magnitude.

In practice, however, experimental investigation of phase behavior of polymer blends and solutions has revealed major deviations from the predictions of the F−H regular solution model. First, effective χ values extracted from small-angle neutron scattering (SANS) studies on blends and block copolymers using the random phase approximation (RPA)[20] are typically not purely enthalpic in nature, but rather display a temperature dependence of the type

$$\chi = A + B/T \qquad (6)$$

where B is the enthalpic term related to $\Delta\epsilon$, and the constant term A is given an entropic origin. Note that in some cases this entropic contribution has been found to account for more than half the effective χ value.[21−23] Second, apparent deviations from a geometric average for the cross-interaction energy ϵ_{AB} have been reported for several polymer mixtures and solutions.[24,25] Finally, and perhaps most importantly, the F−H incompressible model fails to predict phase separation upon heating through the inverted miscibility gap (LCST), which has been systematically observed for miscible or marginally miscible polymer mixtures and solutions.[1,2] A straightforward thermodynamic analysis of LCST-type phase behavior shows that both the enthalpy and entropy changes upon demixing at elevated temperatures must be positive.[26] In other words, the LCST, in contrast to the classical enthalpically driven UCST, results from an increase in entropy at high temperatures in the phase-separated state compared to the miscible state.[26] Moreover, phase separation upon heating through the LCST is always accompanied by a finite volume expansion, which explains the systematic pressure dependence reported for this transition.[27−29] In short, high pressures favor the denser miscible state, thereby raising the cloud point temperature. In contrast, pressure leads to either an increase[30] or decrease[31] of the phase separation transition temperature in UCST-type systems, depending on the sign of the change in volume upon mixing ΔV_{mix}. The incompressible F−H theory equally fails to predict these important effects of pressure on polymer blend compatibility.

The wide body of experimental data on extracted χ values and phase behavior in polymer blends and solutions has led to the development of several theoretical treatments extending the classical Flory−Huggins theory to account for compressibility, pressure effects, and phase separation upon heating. To this end, numerous equation-of-state (EOS) theories[32] have been developed which express the equilibrium density of homopolymers and mixtures as a function of pressure and temperature and further provide an expression for the change in free energy upon mixing compressible fluids. Examples of these compressible thermodynamic treatments include the general corresponding states theory of Prigogine and collaborators,[3] and its modification by Flory, Orwoll, and Vrij,[4] the Sanchez−Lacombe lattice-fluid model,[6,25,26,33] the lattice cluster theory of Dudowicz and Freed,[7] the continuous space EOS of Hino and Prauznits,[8] and the Born−Green−Yvon lattice model of Lipson and co-workers.[9−11] These more rigorous thermodynamic treatments have all shown that, in addition to the relative magnitude of the solubility parameters δ, dissimilarities in the EOS properties of the pure

components, manifest in the variation of homopolymer densities with temperature and pressure, play an important role in determining thermodynamic compatibility in polymer blends and solutions. Unfortunately, while these compressible theories clearly present an improved description of polymer thermodynamics compared to the F−H theory, the price for this increased rigor is an apparent loss of predictive capability and greater mathematical complexity. So far, their use as simple thermodynamic tools for phase diagram prediction has thus been very limited.

Aware of the necessity for such a tool, we recently derived a simple model for the free energy of mixing of weakly interacting polymer blends and solutions that extends the classical regular solution model to account for thermal expansion.[34] Albeit less rigorous than the compressible theories developed to date, this model has the benefit of depending only on the pure component properties of mass density, solubility parameter, and thermal expansion coefficient, which are either available in the literature or can be readily calculated or simulated. We recently illustrated its use by predicting, at least qualitatively, spinodal curves for a series of polystyrene/poly *n*-alkyl methacrylate blends.[34] In this paper, the model is further applied to a much wider range of blend chemistries spanning polyolefin mixtures, characterized by segmental interactions of a purely dispersive nature, to mixtures containing more polar components such as polycarbonates, poly(ethylene oxide), polycaprolactone, etc. The ability to qualitatively predict the phase behavior of each of these systems is illustrated and discussed. In the following section, we first summarize the derivation of the free energy expression.

I. Compressible Regular Solution Model

To proceed, we consider the mixing of n_A and n_B chains of two compressible homopolymers A and B, comprising N_A and N_B segments of hard core (zero kelvin, zero pressure) volume v_A and v_B, respectively. At this assumed hard core state, the total volumes occupied by each pure component, $V_{i,hc}$, and the mixture, V_{hc}, are simply given by

$$V_{i,hc} = n_i N_i v_i$$
$$V_{hc} = n_A N_A v_A + n_B N_B v_B \tag{7}$$

According to the definition of reduced properties typically used in EOS theories,[32] the actual volumes V_i, $i =$ A, B, occupied by the pure compressible fluids at any temperature T and pressure P are related to the hard core volumes through the reduced densities $\tilde{\rho}_A$ and $\tilde{\rho}_B$, respectively:

$$\tilde{\rho}_i(T,P) = \frac{V_{hc,i}}{V_i} = \frac{n_i N_i v_i}{V_i} = \frac{\rho_i}{\rho_i^*} \tag{8}$$

where ρ_i is the T- and P-dependent mass density and $\rho_i^* = M_{u,i}/N_0 v_i$ is the hard core density, given by the ratio of the segment molecular weight $M_{u,i}$ (g/mol) and hard core volume (N_0 is Avogadro's number). The reduced density $\tilde{\rho}_i$ is simply a measure of the fractional occupied volume or, equivalently, one minus the "fractional free volume" in the compressible fluid. Likewise, the total volume V occupied by the mixture at T and P is related to the mixture reduced density $\tilde{\rho}$ and the total hard core volume V_{hc}:

$$\tilde{\rho}(T,P) = \frac{V_{hc}}{V} = \frac{n_A N_A v_A + n_B N_B v_B}{V} = \frac{\rho}{\rho^*} \tag{9}$$

where ρ and ρ^* are the mixture density and hard core density, respectively.

In keeping with the spirit of the well-known Flory−Huggins theory, we consider the change in Gibbs free energy upon mixing, ΔG_{mix}, to arise from the changes in combinatorial entropy and interaction energy. As suggested early on by Hildebrand[35] and Flory,[14] the change in combinatorial entropy upon mixing two compressible components A and B should scale with the logarithms of the ratios of the "free volume" available in the mixture, $V_{f,m}$, to those in the pure components, $V_{f,A}$ and $V_{f,B}$:

$$\Delta S_{comb}/k = n_A \ln\left(\frac{V_{f,m}}{V_{f,A}}\right) + n_B \ln\left(\frac{V_{f,m}}{V_{f,B}}\right) \tag{10}$$

The free volume of component i, $V_{f,i}$, is simply given by the difference between the total volume V_i at T and P and the hard core volume $V_{hc,i}$ and can thus be related to the reduced densities as follows:

$$V_{f,i} = V_i - V_{hc,i} = (1 - \tilde{\rho}_i)V_i \tag{11a}$$

$$V_{f,m} = V - V_{hc,A} - V_{hc,B} = (1 - \tilde{\rho})V \tag{11b}$$

Inserting these relations into eq 10 yields the following expression for the change in combinatorial entropy on mixing, upon simplifications:

$$\Delta S_{comb}/k = -[n_A \ln \phi_A + n_B \ln \phi_B] + \left[n_A \ln\left(\frac{1-\tilde{\rho}}{1-\tilde{\rho}_A}\right) + n_B \ln\left(\frac{1-\tilde{\rho}}{1-\tilde{\rho}_B}\right)\right] \tag{12}$$

where ϕ_i is the volume fraction of component i defined as $V_i/(V_A + V_B)$. In this definition, we have made use of the approximation $V \approx (V_A + V_B)$, since $V_A + V_B$ differs from V only by the small quantity ΔV_{mix}, typically on the order of $10^{-4}V$.

Equation 12 gives a simple expression for the combinatorial entropy gain upon mixing for a binary compressible mixture. It consists of two terms: the classical (incompressible) combinatorial entropy, which scales with the logarithms of the volume fraction of each component, and a second term that arises from compressibility and is related to the difference in free volume between the mixture and the pure components. Hence, if component i undergoes a contraction upon mixing, in which case $(1 - \tilde{\rho})/(1 - \tilde{\rho}_i) < 1$, this will contribute a negative term to the entropy of mixing which destabilizes the mixture in comparison to the incompressible limit.

Still keeping with the spirit of the F−H theory and assuming random mixing (mean field approximation), an equally simple expression can be derived for the change in interaction energy upon mixing. In the pure state, the total interaction energy is obtained by counting the number of pairwise interactions of

type A−A and B−B. Herein, this is done in terms of hardcore cohesive energy densities $\delta_{i,0}^2 = -(1/2)(z\epsilon_{ii}/v_i)$ (energy/vol):

$$E_{\text{pure}} = n_A N_A v_A\left(\frac{1}{2}\frac{z\epsilon_{AA}}{v_A}\right)\frac{n_A N_A v_A}{V_A} + n_B N_B v_B\left(\frac{1}{2}\frac{z\epsilon_{BB}}{v_B}\right)\frac{n_B N_B v_B}{V_B}$$

$$= -n_A N_A v_A \delta_{A,0}^2 \tilde{\rho}_A - n_B N_B v_B \delta_{B,0}^2 \tilde{\rho}_B \quad (13)$$

where ϵ_{ii} is the attractive (negative) segmental interaction energy of the $i-i$ pair and z is the number of nearest-neighbor monomers in the pure melts. For the sake of generality, an alternate "off-lattice" derivation for ΔE_{mix} is also provided in Appendix A1. The dilution factors $\tilde{\rho}_i$ multiplying the self-interaction energy terms reflect the reduced probability of segmental interactions in the pure compressible melts compared to the hard core state (incompressible limit). The interaction energy in the mixed state can be calculated in a similar fashion, making use of the classical regular solution model approximation[17] for the cross-interaction energy density $\delta_{AB,0}^2$:

$$\delta_{AB,0}^2 = \frac{1}{2}\frac{z\sqrt{\epsilon_{AA}\epsilon_{BB}}}{\sqrt{v_A v_B}} = \delta_{A,0}\delta_{B,0} \quad (14)$$

yielding

$$E_{\text{mixed}} = -n_A N_A v_A \delta_{A,0}^2 \phi_A \tilde{\rho}_A - n_B N_B v_B \delta_{B,0}^2 \phi_B \tilde{\rho}_B - 2n_A N_A v_A \delta_{A,0}\delta_{B,0}\phi_B\tilde{\rho}_B \quad (15)$$

Again, the dilution factor $\phi_i\tilde{\rho}_i = n_i N_i v_i/V$ represents the reduced probability of interacting with a segment of type i in the compressible mixed state compared to the hard core state.

From eq 13 and eq 15, a very simple perfect square is obtained for the change in interaction energy per unit volume, $\Delta E_{\text{mix}}/V$:

$$\frac{\Delta E_{\text{mix}}}{V} = \phi_A\phi_B\tilde{\rho}_A^2\delta_{A,0}^2 + \phi_A\phi_B\tilde{\rho}_B^2\delta_{B,0}^2 - 2\phi_A\phi_B\tilde{\rho}_A\tilde{\rho}_B\delta_{A,0}\delta_{B,0}$$

$$= \phi_A\phi_B(\tilde{\rho}_A\delta_{A,0} - \tilde{\rho}_B\delta_{B,0})^2 \quad (16)$$

Note that, alternatively, eq 16 can be rewritten in a more transparent form that effectively separates the compressible and incompressible contributions to the change in interaction energy:

$$\frac{\Delta E_{\text{mix}}}{V} = \phi_A\phi_B\tilde{\rho}_A\tilde{\rho}_B(\delta_{A,0} - \delta_{B,0})^2 + \phi_A\phi_B(\tilde{\rho}_A - \tilde{\rho}_B)(\delta_A^2 - \delta_B^2) \quad (16a)$$

where $\delta_i^2 = \tilde{\rho}_i\delta_{i,0}^2$ is the T- and P-dependent cohesive energy density. Hence, similar to the change in combinatorial entropy upon mixing, the expression for the change in interaction energy for the compressible mixture contains two terms. The first term in eq 16a is the classical exchange interaction energy, diluted by the factors $\tilde{\rho}_i$. It can be related back to the Flory−Huggins interaction energy via the approximation

$$\chi^{\text{FH}} = \frac{\sqrt{v_A v_B}}{kT}(\delta_{A,0} - \delta_{B,0})^2 \quad (17)$$

The second term in eq 16a, *which can be either positive or negative*, arises from the dilution or concentration of self-interactions (ϵ_{ii}) upon mixing. Hence, if component B is characterized at the same time by a larger free volume ($\tilde{\rho}_A > \tilde{\rho}_B$) as well as stronger self-interactions ($\delta_B^2 > \delta_A^2$) than component A, the contraction this component will undergo upon mixing is energetically favorable.

Combining eqs 12 and 16a, the total change in free energy per unit volume, Δg_{mix}, at atmospheric pressure ($P\Delta V_{\text{mix}}$ term ignored) is given by

$$\Delta g_{\text{mix}} = kT\left[\frac{\phi_A\tilde{\rho}_A}{N_A v_A}\ln\phi_A + \frac{\phi_B\tilde{\rho}_B}{N_B v_B}\ln\phi_B\right] + \phi_A\phi_B\tilde{\rho}_A\tilde{\rho}_B(\delta_{A,0} - \delta_{B,0})^2 + \phi_A\phi_B(\tilde{\rho}_A - \tilde{\rho}_B)(\delta_A^2 - \delta_B^2) \quad (18)$$

In this expression, the second entropy term of eq 12 has been neglected, since it can be readily shown that it is orders of magnitude smaller than the leading terms. This yields a simplified expression for Δg_{mix}, which contains three terms: the first term is the classical combinatorial entropy of mixing, while the second term is the classical regular solution model exchange interaction energy, both diluted compared to the incompressible limit. The third term arises from the very fact that the mixture is compressible, thus accounting for equation-of-state effects**.** Although common to other compressible theories developed to date, this extra contribution to the free energy of mixing has been expressed here as a function of *pure component properties only*, namely the reduced density and cohesive energy density or solubility parameter. This yields a compressible free energy expression that can be used as a *predictive* thermodynamic tool.

Although written in its simplest form, the free energy expression of eq 18 does not provide, as is, transparent expressions for the *total* changes in entropy, enthalpy, and volume upon mixing, ΔS_{mix}, ΔH_{mix}, and ΔV_{mix}. For example, the first term of eq 18 is only the combinatorial part of the change in entropy upon mixing, which should further include nonideal contributions arising from compressibility. These total changes per unit volume can be readily calculated, however, using standard thermodynamic relations.[36] Indeed, the total change in entropy per volume Δs_{mix} can be obtained from the derivative of Δg_{mix} with respect to temperature:

$$\Delta s_{\text{mix}} = -\left.\frac{\partial\Delta g_{\text{mix}}}{\partial T}\right|_{P,\phi_i} \quad (19)$$

Likewise, the fractional change in volume upon mixing, $\Delta V_{\text{mix}}/V$, is obtained from the derivative of the Gibbs free energy with respect to pressure:

$$\frac{\Delta V_{\text{mix}}}{V} = \left.\frac{\partial\Delta g_{\text{mix}}}{\partial P}\right|_{T,\phi_i} \quad (20)$$

Finally, the change in enthalpy upon mixing per unit volume, Δh_{mix}, is simply given by

$$\Delta h_{mix} = \Delta g_{mix} + T\Delta s_{mix} = \Delta g_{mix} - T\left.\frac{\partial \Delta g_{mix}}{\partial T}\right|_{P,\phi} \quad (21)$$

Approximate expressions for these thermodynamic quantities at atmospheric (∼zero) pressure are derived in Appendix A2.

For a compressible binary mixture, phase stability requires that the system be stable with respect to both composition and volume fluctuations.[4,5,26,33] When the Gibbs free energy per unit volume is used, this translates into the following mathematical expression for the stability condition:[26,33]

$$g_{\phi\phi} = \left.\frac{\partial^2 \Delta g_{mix}}{\partial \phi_A{}^2}\right|_{T,P} = \left.\frac{\partial^2 \Delta g_{mix}}{\partial \phi_A{}^2}\right|_{T,P,\tilde{\rho}} - \tilde{\rho}_B\left(\left.\frac{\partial^2 \Delta g_{mix}}{\partial \tilde{\rho}\,\partial \phi_A}\right|_{T,P}\right)^2 > 0 \quad (22)$$

However, since the simplified free energy expression given by eq 18 only depends on pure component variables and not on $\tilde{\rho}$, the second term of eq 22 is equal to zero. At atmospheric pressure, spinodal temperatures can thus be readily calculated using the stability criterion for the mixed state obtained from the following second derivative of the intensive free energy with respect to composition:

$$g_{\phi\phi} = \left.\frac{\partial^2 \Delta g_{mix}}{\partial \phi_A{}^2}\right|_{T,P} \approx \left.\frac{\partial^2 \Delta g_{mix}}{\partial \phi_A{}^2}\right|_{T,P,\tilde{\rho}}$$

$$= kT\left[\frac{\tilde{\rho}_A}{\phi_A N_A v_A} + \frac{\tilde{\rho}_B}{\phi_B N_B v_B}\right] - 2\tilde{\rho}_A\tilde{\rho}_B(\delta_{A,0} - \delta_{B,0})^2 - 2(\tilde{\rho}_A - \tilde{\rho}_B)(\delta_A{}^2 - \delta_B{}^2) > 0 \quad (23)$$

while at the spinodal, $g_{\phi\phi}$ equals zero.

II. Phase Behavior Predictions and Discussion

II.1. Pure Component Properties. In the next sections, the stability criterion given by eq 23 is employed to predict phase behavior for a series of weakly interacting polymer pairs spanning systems characterized by purely dispersive attractions to more polar homopolymers such as poly(ϵ-caprolactone), most of which have been investigated experimentally by other authors. To do so, the following pure component properties were determined from experimental $P-V-T$ data[32] and group contribution calculations:[19] ρ_i*, $\tilde{\rho}_i(T,P)$, and $\delta_i(T,P)$.

The hard core and reduced densities were obtained in the following manner. $P-V-T$ data are available in the literature for many homopolymers over a certain T range, typically in the form of empirical Tait equation fits to the specific volume, $1/\rho$ (see for example ref 32 which reviews $P-V-T$ properties for 56 homopolymers). Setting $P = 0$ in such fits provides a simulated data set for ρ as a function of temperature. The hard core density and thermal expansion coefficient were computed by fitting these "data" (or actual data) from the melt-state regime to the following form:

$$\rho_i(T) = \rho_i^* \exp(-\alpha_i T) \quad (24)$$

Table 1. Parameters Used for Spinodal Predictions

homopolymer	ρ^* (g/cm^3)	α (10^{-4} K^{-1})	$\delta(298)$ (J$^{1/2}$/cm$^{3/2}$)	$N_{av}v$ (cm^3/mol)
PS	1.24	5.13	18.19	83.96
PCHMA	1.36	6.24	18.70	123.48
PVME	1.25	6.65	18.50	46.36
PPO	1.45	7.23	18.90	83.04
PαMS[a]	1.33	5.76	18.50	86.88
PEMA	1.42	7.47	19.00	80.09
PEA	1.39	7.24	19.56	71.85
PB[b]	1.06	5.67	16.20	50.98
PI[b]	1.09	6.51	16.40	62.62
PIB[c]	1.08	5.65	18.50	51.59
P(E-*r*-B)66[c]	1.14	7.10	18.71	49.21
P(E-*r*-B)97[c]	1.06	6.78	18.10	52.82
PE[d]	1.10	8.11	18.50	25.38
PEE[d]	1.10	7.79	16.47	50.70
PEP[d]	1.11	8.00	17.80	31.66
PMMA	1.42	5.48	19.65	70.42
PCL	1.32	6.39	19.66	86.64
PC	1.50	6.21	19.47	168.85
SAN6	1.28	5.92	18.6	76.65
SAN18	1.30	5.70	19.52	68.06
SAN40	1.31	5.16	21.57	57.40
PEO	1.38	7.09	21.30	31.79
PVC	1.79	7.40	21.73	35.09

[a] $P-V-T$ data from ref 52. [b] $P-V-T$ data from ref 97. [c] $P-V-T$ data and solubility parameters from ref 18. [d] $P-V-T$ data and solubility parameters from ref 98.

where a constant α_i (the best fit melt state value) was used as a first approximation. This procedure yields ρ_i* and hence $v_i = M_{u,i}/N_0\rho_i$*, the hard core segmental volume. The reduced density $\tilde{\rho}_i(T)$ is then given by the actual density $\rho_i(T)$ divided by ρ_i*. A similar approach was used to determine the temperature-dependent solubility parameters. The values of $\delta_i(298)$, calculated using group contributions according to van Krevelen at 25 °C, were extrapolated to other temperatures in the following manner:

$$\delta_i{}^2(T) = -\frac{1}{2}\frac{z\epsilon_{ii}\rho_i(T)}{v_i} = \delta_i{}^2(298)\left(\frac{\tilde{\rho}_i(T)}{\tilde{\rho}_i(298)}\right) \quad (25)$$

The homopolymer values of α_i, ρ_i*, $\delta_i(298)$, and v_i used to compute the spinodal diagrams presented in the next sections are listed in Table 1. In computing these spinodal diagrams, homopolymer molecular weights were chosen to match those used in experimental studies, thereby allowing for comparison with reported cloud point curves near the critical point. While the primary goal of this work was to demonstrate the qualitative, rather than quantitative, predictive capability of the model, these cloud point curves were added to figures shown below. For those systems for which no cloud point data are available, homopolymer molecular weights, taken as equal for the two blend components, were chosen such that the predicted critical point would fall within an experimentally accessible T range. It is important to note that *no adjustable parameters* were used to compute any of the diagrams shown in the remainder of this paper, since Berthelot's mixing rule was assumed to calculate the exchange interaction energy.

II.2. Polystyrene-Based Blends. In this section, we start by considering six polystyrene-based blends which have been the subject of extensive experimental investigation. These include four well-known miscible pairs: polystyrene/poly(vinyl methyl ether),[37−45] denoted PS/PVME, polystyrene/poly(cyclohexyl methacrylate),[46−48]

denoted PS/PCHMA, polystyrene/poly(2,6-dimethylphenylene oxide),[49−51] denoted PS/PPO, and polystyrene/poly(α-methylstyrene),[52,53] denoted PS/PαMS. Even though these four blends form homogeneous mixtures over extended temperature ranges even for reasonably large homopolymer molecular weights, they differ in that the first three systems phase separate upon heating through a LCST, while the latter only exhibits UCST-type phase behavior at experimentally accessible temperatures. Both the large degree of thermodynamic compatibility and the respective trends in phase behavior reported for each of these four systems are successfully captured by the predicted spinodal curves shown in Figure 2a−d. Hence, PS/PVME, PS/PCHMA, and PS/PPO are predicted to display both LCST- and UCST-type transitions, although the extremely low temperature of the latter prevents its experimental observation. In contrast, PS/PαMS is correctly predicted to just display UCST-type phase behavior, only observable for high molecular weights. Spinodal diagrams were also calculated for two well-known immiscible PS-based blends, namely, PS/polybutadiene[54] (PS/PB) and PS/polyisoprene[55] (PS/PI), shown in Figure 2e,f. Although the model tends to overestimate their degree of incompatibility, the thermodynamics of these systems is also successfully captured. Hence, UCST-type spinodals are predicted, only observable at experimentally accessible temperatures for very low molecular weights of these immiscible components (∼2000 g/mol).

The qualitative agreement between the calculated spinodal diagrams shown in Figure 2 and the experimentally observed phase behavior is excellent, implying that the compressible regular solution model presented here is predictive for these weakly interacting systems. Moreover, computing the relations for Δs_{mix} and Δh_{mix} according to eq A2.3 and eq A2.5 of Appendix A2 clearly reveals the drastically different thermodynamic origin of the two types of transitions observed in these blends. This is illustrated in Figure 3, where Δg_{mix}, Δh_{mix}, and $T\Delta s_{mix}$ are given as a function of temperature for the 100K/100K blend of PS and PCHMA containing 50% PS. Thus, phase separation (demixing) upon cooling through the *enthalpically driven* UCST is, as anticipated, accompanied by a favorable decrease in the blend enthalpy ($\Delta h_{mix} > 0$, $\Delta h_{demix} < 0$) and unfavorable, but smaller in magnitude, decrease in the blend entropy ($\Delta s_{mix} > 0$, $\Delta s_{demix} < 0$). In contrast, phase separation upon heating through the *entropically driven* LCST is accompanied by a favorable increase in the blend entropy ($\Delta s_{mix} < 0$, $\Delta s_{demix} > 0$) and unfavorable, but smaller in magnitude, increase in the blend enthalpy ($\Delta h_{mix} < 0$, $\Delta h_{demix} > 0$). The increase in the system entropy upon phase separation at high temperatures through the LCST in these miscible blends is, as expected, also accompanied by a small volume expansion since a negative $\Delta V_{mix}/V$ of $\sim -2 \times 10^{-4}$ to -8×10^{-4} is computed using eq A2.4 of Appendix A2. This is again illustrated for the PS/PCHMA pair in Figure 4a−c, where $\Delta V_{mix}/V$, Δg_{mix}, Δh_{mix}, and $T\Delta s_{mix}$ are shown, this time as a function of composition and for two temperatures, above (673 K) and below (523 K) the LCST, respectively.

More importantly, when applied to the series of blends considered in Figure 2, the model further provides a very simple explanation for the molecular origin of phase behavior in each of these weakly interacting systems. Indeed, whenever the exchange interaction energy scaling as $(\delta_{A,0} - \delta_{B,0})^2$ is large, which is the case, e.g., for styrene and isoprene, the second term of eq 18 governs the free energy of mixing, and the system displays classical UCST-type phase behavior. The actual transition, however, is only observable for low molecular weights where the small combinatorial entropy of mixing (first term of eq 18) overcomes the unfavorable enthalpic interactions between the unlike segments. In contrast, when the exchange interaction energy is small, i.e., whenever the two weakly interacting components have sufficiently similar solubility parameters[17] or mass densities,[56] the third term of eq 20 tends to govern the free energy of mixing and its variation with temperature. At low temperatures and under certain conditions, this contribution to the free energy, which arises from differences in the pure components' free volumes and cohesive energy densities, can be negative, promoting mixing. This favorable situation arises whenever the more cohesive (larger δ) homopolymer is also the one with a larger degree of free volume (lower $\tilde{\rho}$) and larger thermal expansion coefficient α. At low temperature, the contraction this component undergoes upon mixing is accompanied by an energetically favorable strengthening of its self-interactions. Upon heating, however, the cohesive energy density of this component decreases at a faster pace than that of the second component, due to its larger α. Given this difference in pure component thermal expansion coefficients, there is always a temperature above which the third term of eq 18 becomes positive, destabilizing the mixed state. This temperature is greatly dictated by the relative magnitude of the two components' thermal expansion coefficients, being lowest for the largest differences. Besides the requirement that the exchange interaction energy $(\delta_{A,0} - \delta_{B,0})^2$ be small enough, a second condition for the experimental observation of the LCST, i.e., at an experimentally accessible temperature, is thus recovered:[5] the two homopolymers must have sufficiently different thermal expansion coefficients. Indeed, if these parameters are too similar, the LCST lies at a temperature exceeding by far the degradation temperature of the polymer components. Such a difference in thermal expansion coefficients is found for blends of PS ($\alpha_{PS} = 5.3 \times 10^{-4}$ K^{-1}) and several chemically distinct homopolymers with which it is reported miscible, namely, PVME ($\alpha_{PVME} = 6.65 \times 10^{-4}$ K^{-1}), PCHMA ($\alpha_{PCHMA} = 6.24 \times 10^{-4}$ K^{-1}), and PPO ($\alpha_{PPO} = 7.2 \times 10^{-4}$ K^{-1}), but also poly(cyclohexyl acrylate), PCHA, poly(tetramethyl carbonate) (TMPC), etc. In contrast, the chemically similar PS and PαMS homopolymers have thermal expansion coefficients of comparable magnitude: 5.13×10^{-4} and 5.76×10^{-4} K^{-1}, respectively. Consequently, in this case, the third term of eq 18 not only is smaller in magnitude but also becomes positive only at extremely high temperatures, ruling out the experimental observation of an inverted coexistence curve for this compatible system. Instead, the competition between a small positive exchange interaction energy (second term of eq 18) and a small negative contribution from EOS effects (third term of eq 18) results in the reported low-T UCST-type phase behavior.

II.3. Chemically Similar Blends. To better illustrate these considerations, the predicted phase behavior of two other chemically similar blends is presented here. Although miscibility might typically expected for these blends, both types of phase behavior (LCST or UCST) are in fact observed, depending on the particular polymer pair. Hence, similar to the PS/PαMS system,

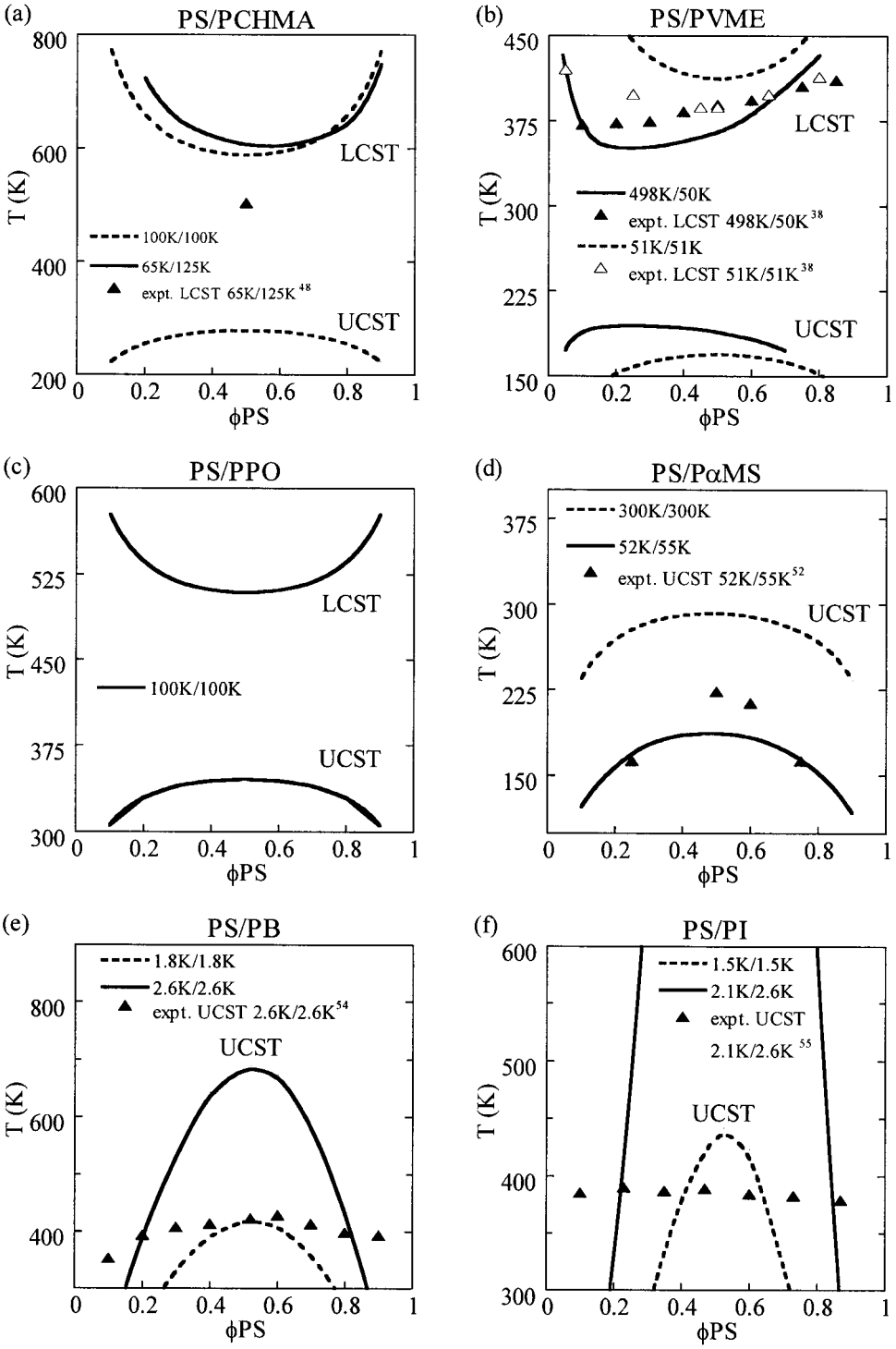

Figure 2. Predicted spinodal diagrams and experimental cloud points for blends of (a) PS/PCHMA, (b) PS/PVME, (c) PS/PPO, (d) PS/PαMS, (e) PS/PB, and (f) PS/PI. The homopolymer molecular weights corresponding to each spinodal or experimental cloud point curve are indicated as follows: *X*K = *X*000 g/mol.

blends of poly(ethyl methacrylate), PEMA, and poly(ethyl acrylate), PEA, are reported to display UCST-type behavior, though with a much lower degree of thermodynamic compatibility.[57] This trend is successfully predicted in the spinodal diagram shown in Figure 5a. In contrast, LCST-type spinodal behavior is predicted for the polybutadiene/polyisoprene (PB/PI) pair, as shown in Figure 5b. Such behavior was in fact recently reported for a 450 000 (450K) g/mol block copolymer of these two components containing 31 wt % PB, which displays a lower disorder/order transition (LDOT) at ~135 °C.[58]

Interestingly, the common difference between the two components in each of these systems is the replacement of a hydrogen atom by a methyl (CH_3) group. For the PS/PαMS or PEA/PEMA pairs, this small chemical variation is accompanied by a modest (~3−5%) increase in the thermal expansion coefficient ($\alpha_{PS} = 5.13$ and $\alpha_{P\alpha MS} = 5.76 \times 10^{-4}$ K^{-1}, $\alpha_{PEA} = 7.24$ and $\alpha_{PEMA} = 7.47 \times 10^{-4}$ K^{-1}). In contrast, the extra CH_3 in polyisoprene results in a much larger (15%) value of α compared to that of polybutadiene ($\alpha_{PB} = 5.67$ and $\alpha_{PI} = 6.56 \times 10^{-4}$ K^{-1}). In the context of the compressible regular solution model presented here, this subtle effect of monomer

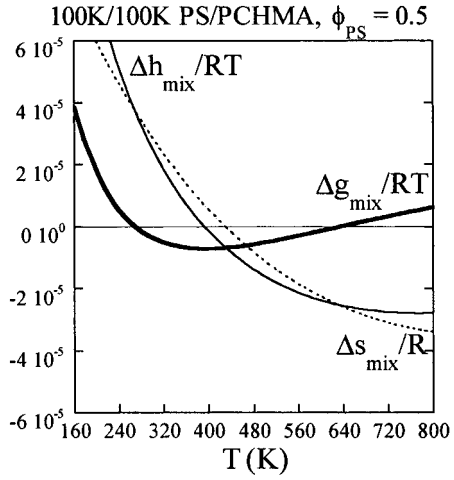

Figure 3. Changes in Gibbs free energy, Δg_{mix}, enthalpy, Δh_{mix}, and entropy, Δs_{mix}, per unit volume as a function of temperature for a 100K/100K PS/PCHMA blend containing 50% PS.

structure on pure component $P-V-T$ properties naturally translates into a tendency for this system to phase separate upon heating.

II.4. Polyolefin Blends. In light of the results presented so far, the explanation for some unusual experimental observations on blends consisting entirely of saturated polyolefins such as polyethylene, polypropylene, polyisobutylene, polybutene, etc., becomes transparent. Owing to their commercial importance, polyolefin blends have been the subject of extensive experimental[18,59−67] and theoretical[23,68−77] investigations, which have unveiled important effects of monomer structure on blend thermodynamics. While most such blends phase separate upon cooling through a classical UCST, some remarkable exceptions have been identified,[63,67] one of which is the reported LCST for most blends of polyisobutylene (PIB) with other saturated polyolefins.[63] Using eq 18, however, the "anomalous" LCST for blends involving PIB becomes predictable and entirely explicable. Indeed, experimental $P-V-T$ data[18,32] show that PIB is characterized by a very small thermal expansion coefficient ($\alpha_{PIB} \sim 5.65 \times 10^{-4}$ K^{-1}) compared to most other saturated polyolefins ($\alpha \sim (7-8) \times 10^{-4}$ K^{-1}). Again, this provides the right conditions for LCST behavior in blends involving this homopolymer and other saturated polyolefins with comparable solubility parameters and mass densities. Examples of such components include head-to-head polypropylene (hhPP) as well as certain random copolymers of ethylene and butene, denoted P(E-*r*-B), obtained upon hydrogenation of polybutadiene. The predicted spinodal diagrams for blends of PIB and two P(E-*r*-B) containing 66 and 97 wt % of butene, respectively, are shown in Figure 6a. Experimentally, it is found that, while the former is miscible at room temperature and displays a LCST at ~100 °C for $M_{wPIB} \sim 81\,000$ (81K) g/mol and $M_{wP(E-r-B)66} \sim 114\,000$ (114K) g/mol (M_w = weight-average molecular weight), the latter is always phase separated at 25 °C and higher temperatures, even for molecular weights of $M_w \sim 50\,000$ (50K) g/mol.[63] These thermodynamic trends are well captured by the phase diagrams of Figure 6a, where the LCST's of 70K/70K and 81K/114K blends of PIB/P(E-*r*-B)66 and a 13K/13K blend of PIB/P(E-*r*-B)97 are shown. Interestingly, the actual transition in PIB/P(E-*r*-B)97 is predicted to lie below room temperature even for low molecular weights of these components, correlating well with the experimental observation of immiscibility at all temperatures for this system.

In contrast to the systems involving polyisobutylene, blends[64] and block copolymers[78,79] of polyethylene and various branched polyolefins such as poly(ethylethylene), PEE, and poly(ethylenepropylene), PEP, are typically incompatible and exhibit phase separation upon cooling through a classical UCST observable for small to intermediate homopolymer molecular weights. The thermodynamic trends of these more classical systems are also successfully predicted by the computed diagrams shown in Figure 6b−d for PE/PEE, PEE/PEP, and PE/PEP blends. For the sake of comparison and in the absence of blend cloud point data, upper disorder/order transitions (UDOT) measured by Bates and co-workers on symmetric block copolymers of these three systems are also shown. Within the framework of the random phase approximation (RPA),[20] these roughly correspond to "equivalent cloud points" for blends of homopolymers of molecular weight $M_n \sim M_{n,\text{block copolymers}}/5.25$. Although no quantitative agreement is claimed, note that the model also correctly predicts the order of increasing miscibility among these three systems.

II.5. PMMA, PC, and PCL-Based Blends. In this section, we further apply eq 18 to blends involving more polar homopolymers such as poly(methyl methacrylate) (PMMA), poly(ϵ-caprolactone) (PCL), and polycarbonate (PC). The compatibilization of PS with each of these homopolymers through random copolymerization of styrene with a more cohesive monomer such as acrylonitrile (AN) has been extensively investigated.[80−86] For example, it is well-known that PMMA is miscible with styrene/acrylonitrile random copolymers, denoted SAN, containing 10−38 wt % acrylonitrile, and the corresponding blends phase separate upon heating through the LCST.[80−82] When the SAN copolymers contain less or more AN, however, immiscibility and the classical UCST behavior are recovered. Parts a and b of Figure 7 show the predicted spinodal diagrams for blends of PMMA and three SAN copolymers containing 6 (SAN6), 18 (SAN18), and 40 wt % acrylonitrile (SAN40), respectively. For comparison, experimental cloud points, only available for highly polydisperse PMMA/SAN18 blends of molecular weights $M_{w,PMMA} \sim 105\,000$ (105K) g/mol and $M_{w,SAN18} \sim 180\,000$ (180K), are also shown. For 18 wt % AN, which is within the reported miscibility window, the model correctly predicts a large degree of thermodynamic compatibility and both a LCST and a UCST, although only the former lies in an experimentally accessible T range. In contrast, both PMMA/SAN6 and PMMA/SAN40 are predicted to be immiscible and to exhibit UCST-type phase behavior, only observable for very low molecular weights of these components (7000 and 3000 g/mol, respectively), in accord with experimental observations. Similar miscibility windows spanning 8−28 and ~15−25 wt % AN, respectively, have been reported for blends of PCL/SAN[83,84] and PC/SAN.[85,86] These trends are also successfully predicted, as seen in the spinodal diagrams shown in Figure 7c−f.

Marginal compatibility and the LCST are also predicted for intermediate molecular weight (50 000 or 50K g/mol) blends of PMMA and PC, as shown in Figure 8a. Although actual cloud point temperatures are not reported, this is in excellent agreement with experi-

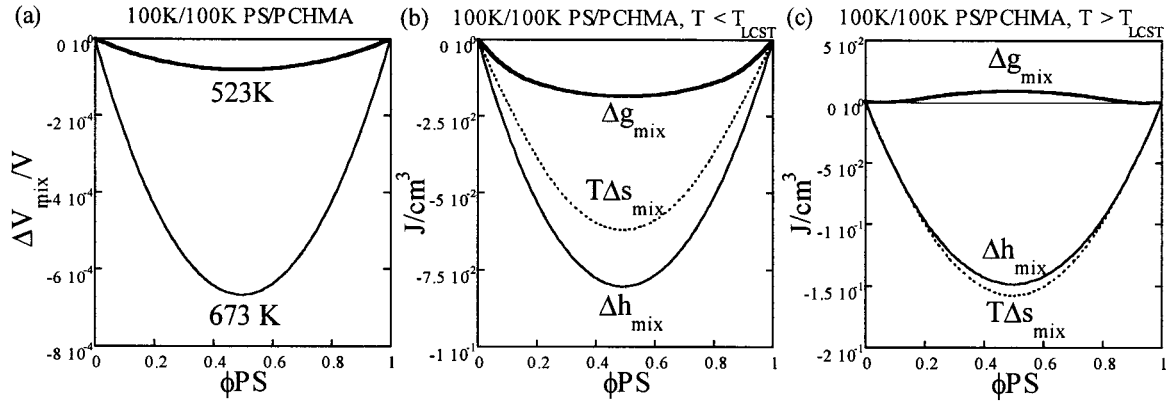

Figure 4. Fractional change in volume on mixing, $\Delta V_{mix}/V$, as a function of composition for 100K/100K PS/PCHMA blend at $T = 523$ K $< T_{LCST} = 600$ K and $T = 623$ K $> T_{LCST}$ (a) and corresponding changes in Gibbs free energy, enthalpy, and entropy per unit volume as a function of composition at (b) 523 K and (c) 623 K.

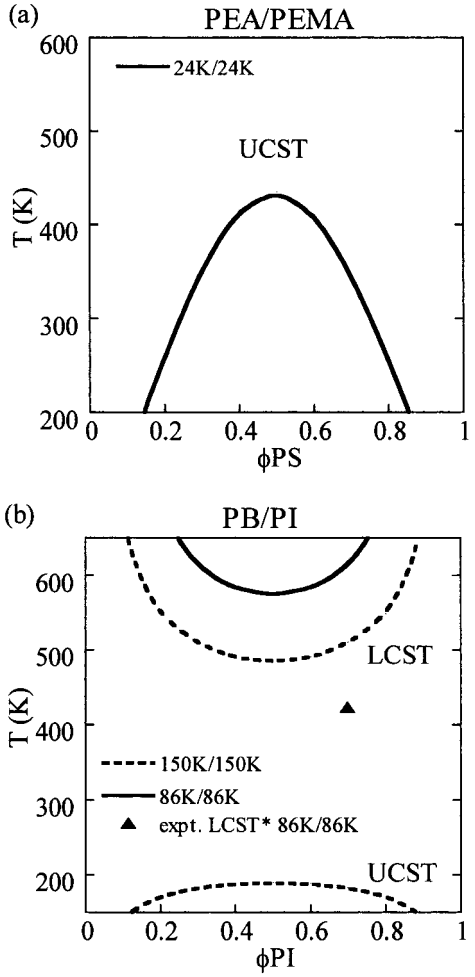

Figure 5. Predicted spinodal diagrams and experimental cloud points for blends of (a) PEMA/PEA and (b) PB/PI. (*) data for 450K PB/PI block copolymer containing 31 wt % PB.[58]

mental studies on this polymer pair, which indicate that the LCST of this blend lies below the glass transition of PC (147 °C) for most commercial molecular weights ($M_w \geq 100\,000$ g/mol).[87−89] A similar type of phase behavior, also shown in Figure 8a, is further predicted for blends of PMMA and PCL. Again, the LCST arises in these systems from a small exchange interation energy (second term of eq 18) combined with a sizable difference in the thermal expansion coefficients of PC and PCL (6.21 and 6.39 $\times$ 10^{-4} K^{-1}, respectively) compared to that of PMMA (5.48 $\times$ 10^{-4} K^{-1}). Moderate miscibility is also predicted for blends of PMMA and poly(ethylene oxide) (PEO), although accompanied by a UCST-type phase behavior for ∼25 000 (25K) g/mol blends of these components. Despite the higher degree of thermodynamic compatibility observed experimentally, the prediction shown in Figure 8b correlates well with the SANS studies of Hopkinson and co-workers. Indeed, these authors reported a decrease in scattering intensity and hence, in the SANS-derived χ parameter, with increasing temperature for PMMA/PEO blends, indicative of UCST-type behavior.[90] Earlier, however, Russell and co-workers also investigated this polymer pair with SANS but reported a roughly constant χ across the whole T range.[91]

II.6. Strongly Interacting Systems. Surprisingly good predictions of phase behavior were obtained for all the systems considered so far using eq 18, which was derived assuming a geometric rule of mixtures for the cross-interaction energy term. This indicates that strong specific interactions do not necessarily need to be invoked to explain the thermodynamics of these systems, even for the more polar systems presented in the last section. This is in contrast, however, to blends involving poly(vinyl chloride), PVC, as well as poly(vinylidene fluoride), PVF_2. Indeed, Berthelot's mixing rule predicts large positive exchange interaction energies (second term of eq 18) and immiscibility for blends of these homopolymers with PMMA, while their miscibility even for high molecular weights has been reported by several authors.[37,92−95] Hence, out of the 25 systems considered in this work, the latter two appear to be the only ones for which a simple geometric average for the cross-interaction energy is wholly unsatisfactory.

Conclusion

A phenomenological free energy expression was derived for compressible polymer mixtures, which extends the classical regular solution model to account for compressibility. This model was derived in a similar fashion as the well-known Flory−Huggins theory, assuming random mixing (mean field approximation). However, in deriving expressions for the change in combinatorial entropy and interaction energy, the free volumes of the pure components and the mixture, defined as the difference between the total and hard core (0 K, zero pressure) volumes, were accounted for. The ability of the model to predict qualitative phase behavior as a function of temperature was demonstrated for homopolymer blends of 23 polymer pairs. Spinodal

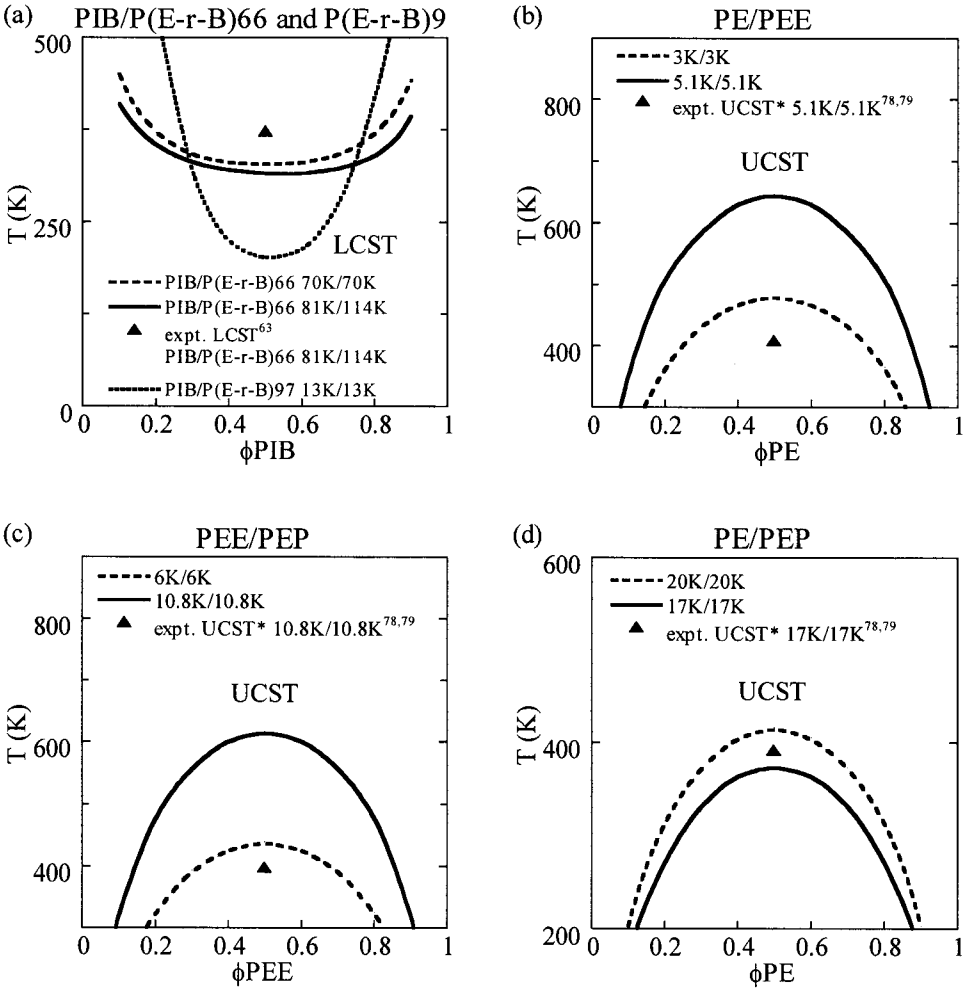

Figure 6. Predicted spinodal diagrams and experimental cloud points for blends of (a) PIB/P(E-*r*-B)X, where *X* is the wt % of butene in the ethylene−butene random copolymer, (b) PE/PEE, (c) PEE/PEP, and (d) PE/PEP. (*) Data for 27K (PE/PEE), 57K (PEE/PEP), and 93K (PE/PEP) symmetric block copolymers.[78,79]

diagrams were calculated for each of these systems, which correlate predictively with their reported phase behaviors. Moreover, surprisingly good quantitative agreement with experimental cloud points near the critical point was obtained, considering that no adjustable parameters were used for the predictions. In computing these spinodal diagrams, the following assumptions were made:

1. The classical regular solution model approximation (Berthelot's mixing rule) was used for the cross-interaction energy density.

2. Hard core and reduced densities of the pure components were obtained by extrapolating experimental $P-V-T$ data to 0 K at 0 pressure (hard core state) assuming *constant thermal expansion coefficients* taken from the melt state.

3. Solubility parameters were obtained using group contributions according to van Krevelen.

The success of eq 18 in predicting phase behavior for so many different polymer pairs, with no adjustable parameters, is a highly encouraging result. Although not attempted here, this compressible regular solution model might also be useful in capturing the phase behavior of block copolymers, ternary and multicomponent blends, block copolymer/homopolymer blends, and possibly polymer solutions, organic small molecule mixtures, or even inorganic mixtures and alloys. In this paper, phase diagrams were only calculated for polymer blend systems for which accurate $P-V-T$ data on the pure components was available in the literature. Provided such data could be measured or simulated, however, we expect that qualitatively accurate phase diagrams could be predicted for numerous additional weakly interacting polymer pairs, including other existing or yet to be studied homopolymer/random copolymer systems besides those based on SAN. One caveat, however, is that while the regular solution model presented here successfully predicts the phase behavior of all the weakly interacting systems considered, erroneous predictions were obtained for systems characterized by stronger specific interactions. PMMA/PVC and PMMA/PVDF were given as two examples of such blends. It is expected that other systems involving strong interactions such as H-bonding and electrostatic interactions would also be poorly described with the model as presented. However, these failures, we believe, mainly point to the inadequacy of a geometric average for cross-interaction energies, rather than a failure of the compressible regular solution model per se, at capturing the thermodynamics of these systems.

Toward the goal of improved quantitative phase diagram predictions, perhaps the most limiting assumption of the list above is that of constant thermal expansion coefficients in extrapolating $P-V-T$ data. While, qualitatively, the predicted phase diagrams and trends in thermodynamic compatibility are unexpect-

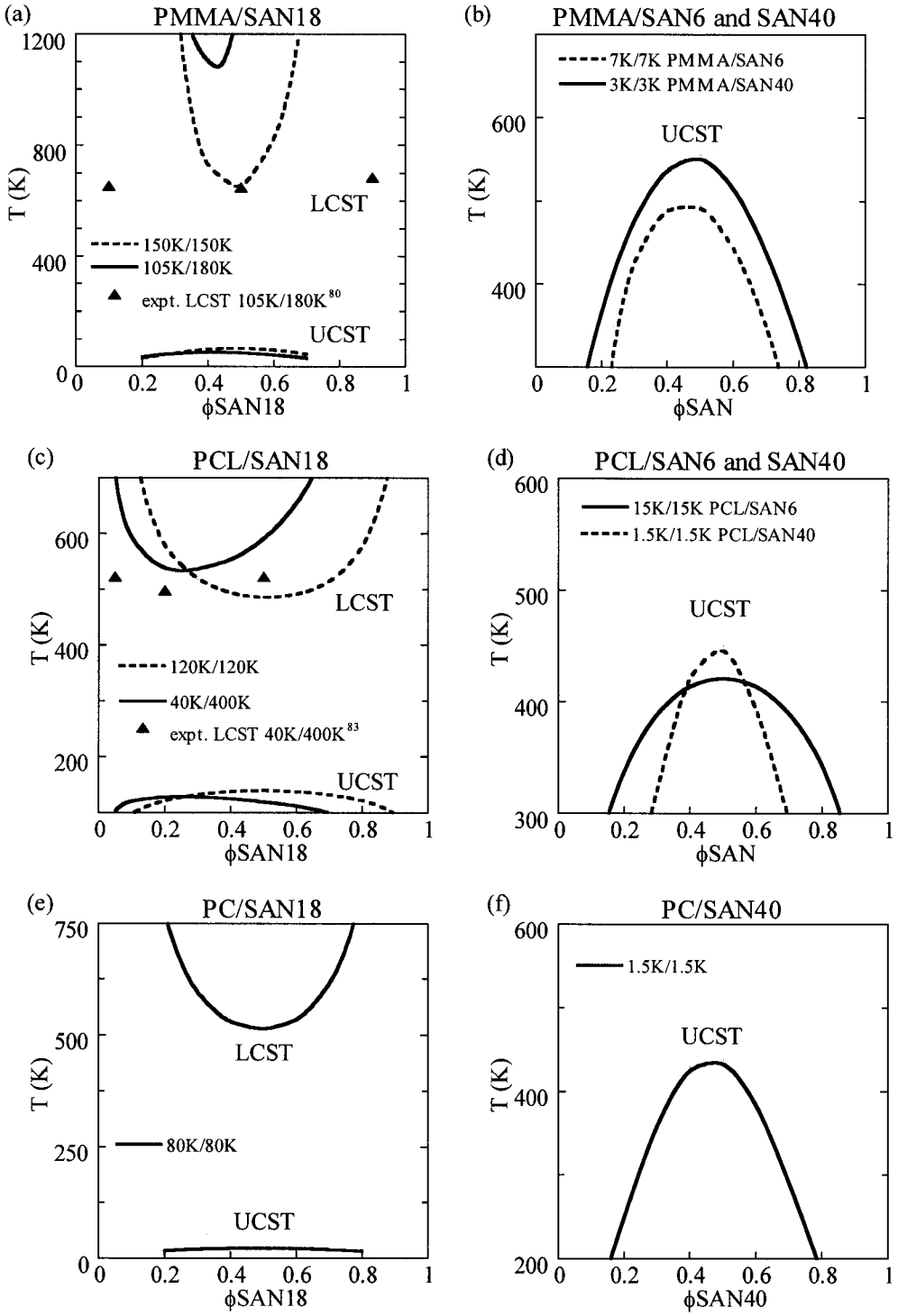

Figure 7. Predicted spinodal diagrams and experimental cloud points for blends of (a, b) PMMA/SANXX, (c, d) PCL/SANX, and (e, f) PC/SANX. In these figures, SANX refers to a styrene/acrylonitrile random copolymer containing *X* wt % acrylonitrile.

edly good, the strong dependence of predicted spinodal temperatures on the values of α suggests that reconsidering this assumption might yield better quantitative agreement with experimental spinodal curves. The sensitivity of the extrapolated values of the hard core parameters and resulting reduced densities on the numerical value of α further supports these conclusions. Besides polydispersity effects, which were not taken into account in the model, another potentially important source of deviations between predictions and experiments is the use of simple group contribution calculations for the evaluation of pure component cohesive energy densities. Indeed, the strong sensitivity of solubility parameter calculations on the particular formalism chosen tends to complicate their use as a quantitative tool. Along these lines, a highly attractive alternative avenue to obtain the pure component thermodynamic parameters necessary for phase diagram predictions using eq 18 or 23 might consist of molecular dynamics and energy minimization simulations. Indeed, Choi et al.[96] recently reported on the use of the commercial software Cerius in combination with the force field UNIVERSAL to simulate the density, cohesive energy density and hard core (0 K) parameters of PS and PVME. These simulated densities and cohesive energy densities, obtained from hypothetical polymer

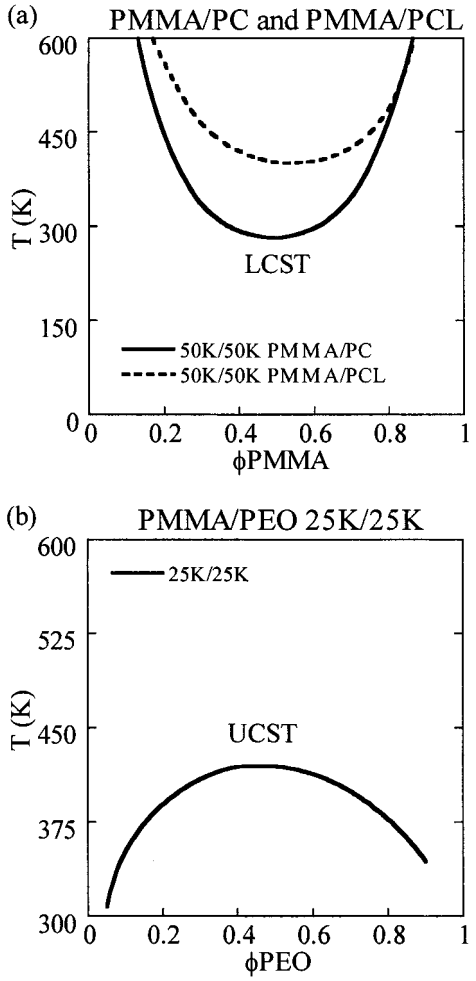

Figure 8. Predicted spinodal diagrams for (a) PMMA/PC and PMMA/PCL blends and (b) PMMA/PEO blends.

chains of as little as 20 segments, were found to be in good agreement with experimentally determined values as well as those obtained from GC calculations. The advantage of this procedure clearly lies in its predictive nature, thereby allowing one to estimate the thermodynamic properties of new and yet to be synthesized polymers, including random copolymers of various compositions. Moreover, this approach might also yield hard core parameters with improved physical meaning in comparison with the extrapolated values used in this work. The potential use of these simulations in combination with the free energy model derived here is currently being investigated.

Finally, besides its use as a simple thermodynamic tool for phase behavior predictions, the phenomenological model derived here further provides a simple explanation for the molecular origin of the inverted coexistence curve (LCST) in compatible polymer blends, solutions, or block copolymers. Indeed, provided the exchange interation energy (second term of eq 18) is small enough, which is achieved for weakly interacting polymer pairs with similar solubility parameters, phase separation upon heating naturally arises from small differences in free volumes and cohesive energy densities between the two components and their increase with rising temperature due to a difference in thermal expansion coefficients. While this concept naturally emerged from most compressible theoretical treatments of polymer thermodynamics, starting with the work of McMaster in 1973,[5] a simple and predictive mathematical expression in terms of pure component properties only is proposed here for the first time.

Acknowledgment. This work was supported in part by an unrestricted grant from the Lord Foundation (A.M.M.) and by the MRSEC program of the National Science Foundation under Award No. DMR 98-08941 (A.M.M.). A.-V. G. Ruzette acknowledges the partial support of IBM and the Belgian and American Educational Foundation. The authors acknowledge the assistance of T. P. Russell in the initial development of this model and helpful discussions with G. Ceder, S. T. Milner, and S. K. Kumar.

Appendix A1

In eq 16, ΔE_{mix} may be alternately derived without reference to a lattice by assuming a van der Waals interaction potential $w_{ij}(r)$ between monomers i and j separated by a distance r, to take the form $w_{ij}(r) = -C_{ij}/r^6$, where C_{ij} is the vdW energy coefficient, having units of energy × vol^2. The total interaction energy E_{ij} for n_iN_i monomers of i interacting with n_jN_j monomers of j in a volume V is given by[100]

$$E_{ij} = \sum_{i,j} \frac{n_i N_i}{2} \int_{\sigma_{ij}}^{\infty} w_{ij}(r)\, \rho_j'(r) 4\pi r^2\, \mathrm{d}r = \sum_{i,j} \frac{n_i N_i}{2} \int_{\sigma_{ij}}^{\infty} \frac{-C_{ij}}{r^6}\, \rho_j'(r) 4\pi r^2\, \mathrm{d}r \quad \text{(A1.1)}$$

where $\rho_j'(r)$ is the local *number* density of j segments, σ_{ij} is an averaged segment hard core diameter, and the system is assumed to be isotropic. Invoking the mean-field approximation $\rho_i'(r) = n_iN_i/V$, and further assuming that $C_{ij} = (C_{ii}C_{jj})^{1/2}$ and $\sigma_{ij} = (\sigma_{ii}\sigma_{jj})^{1/2}$, the integral in eq A1.1 yields

$$E_{ij} = -\sum_{i,j} n_i N_i \frac{2\pi (C_{ii}C_{jj})^{1/2}}{3(\sigma_{ii}\sigma_{jj})^{3/2}} \left(\frac{n_j N_j}{V}\right) \quad \text{(A1.2)}$$

The total interaction energy for the pure state is therefore

$$E_{pure} = E_{pure,A} + E_{pure,B} = -n_A N_A \frac{2\pi C_{AA}}{3{\sigma_A}^3} \left(\frac{n_A N_A}{V_A}\right) - n_B N_B \frac{2\pi C_{BB}}{3{\sigma_B}^3} \left(\frac{n_B N_B}{V_B}\right) \quad \text{(A1.3)}$$

Noting that $\tilde{\rho}_i = n_iN_iv_i/V_i$ and identifying the 0 K cohesive energy density of each component as

$${\delta_{i,0}}^2 = \frac{2\pi C_{ii}}{3{\sigma_{ii}}^3 {v_i}^2} \quad \text{(A1.4)}$$

we can rewrite eq A1.3 as

$$E_{pure} = -n_A N_A v_A {\delta_{A,0}}^2 \tilde{\rho}_A - n_B N_B v_B {\delta_{B,0}}^2 \tilde{\rho}_B \quad \text{(A1.5)}$$

which is identical to eq 13. Similarly, the mixed state energy is given by

$$E_{mixed} = -n_A N_A \frac{2\pi C_{AA}}{{\sigma_A}^3} \left(\frac{n_A N_A}{V}\right) - n_B N_B \frac{2\pi C_{BB}}{{\sigma_B}^3} \left(\frac{n_B N_B}{V}\right) - n_A N_A \frac{2\pi (C_{AA}C_{BB})^{1/2}}{3(\sigma_A\sigma_B)^{3/2}} \left(\frac{n_B N_B}{V}\right) - n_B N_B \frac{2\pi (C_{AA}C_{BB})^{1/2}}{3(\sigma_A\sigma_B)^{3/2}} \left(\frac{n_A N_A}{V}\right) \quad \text{(A1.6)}$$

Setting $\phi_i\tilde{\rho}_i = n_iN_iv_i/V$ and $\delta_{AB,0}{}^2 = \delta_{A,0}\delta_{B,0}$ we obtain

$$E_{mixed} = -n_AN_Av_A\delta_{A,0}{}^2\phi_A\tilde{\rho}_A - n_BN_Bv_B\delta_{B,0}{}^2\phi_B\tilde{\rho}_B - 2n_AN_Av_A\delta_{A,0}\delta_{B,0}\phi_B\tilde{\rho}_B \quad (A1.7)$$

which is equivalent to eq 15. The change in interaction energy upon mixing is then calculated as $\Delta E_{mix} = E_{mixed} - E_{pure}$.

Appendix A2

From the free energy expression given by eq 18, the changes in entropy, enthalpy, and volume upon mixing are readily obtained using standard thermodynamic relationships. To this end, we still assume constant α's and further ignore the negligible variation of the volume fractions ϕ_i with T and/or P. Hence, the only T- and P-dependent parameters in eq 18 are the reduced densities and cohesive energy densities, for which

$$\left.\frac{d\tilde{\rho}_i}{dT}\right|_{P,\phi} = -\alpha_i\tilde{\rho}_i \quad \text{and} \quad \left.\frac{d\tilde{\rho}_i}{dP}\right|_{T,\phi} = \beta_i\tilde{\rho}_i \quad (A2.1)$$

$$\left.\frac{d\delta_i{}^2}{dT}\right|_{P,\phi} = -\alpha_i\delta_i{}^2 \quad \text{and} \quad \left.\frac{d\delta_i{}^2}{dP}\right|_{T,\phi} = \beta_i\delta_i{}^2 \quad (A2.2)$$

where β_i is the isothermal compressibility of component i.

Using these relations yields the following expressions for Δs_{mix} and $\Delta V_{mix}/V$, the change in entropy on mixing per unit volume and the fractional change in volume on mixing:

$$\Delta s_{mix} = -\left.\frac{\partial \Delta g_{mix}}{\partial T}\right|_{0,\phi_i}$$

$$= -k\left[\frac{(1-\alpha_AT)\phi_A\tilde{\rho}_A}{N_Av_A}\ln(\phi_A) + \frac{(1-\alpha_BT)\phi_B\tilde{\rho}_B}{N_Bv_B}\ln(\phi_B)\right] + (\alpha_A+\alpha_B)\phi_A\phi_B\tilde{\rho}_A\tilde{\rho}_B(\delta_{A_0}-\delta_{B_0})^2 - \phi_A\phi_B[(\alpha_B\tilde{\rho}_B-\alpha_A\tilde{\rho}_A)\times (\delta_A{}^2-\delta_B{}^2)] + \phi_A\phi_B[(\tilde{\rho}_A-\tilde{\rho}_B)(\alpha_A\delta_A{}^2-\alpha_B\delta_B{}^2)] \quad (A2.3)$$

and

$$\Delta V_{mix}/V = \left.\frac{\partial \Delta g_{mix}}{\partial P}\right|_{T,\phi}$$

$$= kT\left[\frac{\beta_A\phi_A\tilde{\rho}_A}{N_Av_A}\ln(\phi_A) + \frac{\beta_B\phi_B\tilde{\rho}_B}{N_Bv_B}\ln(\phi_B)\right] + (\beta_A+\beta_B)\phi_A\phi_B\tilde{\rho}_A\tilde{\rho}_B(\delta_{A_0}-\delta_{B_0})^2 + \phi_A\phi_B[(\beta_A\tilde{\rho}_A-\beta_B\tilde{\rho}_B)\times (\delta_A{}^2-\delta_B{}^2)] + \phi_A\phi_B[(\tilde{\rho}_A-\tilde{\rho}_B)(\beta_A\delta_A{}^2-\beta_B\delta_B{}^2)] \quad (A2.4)$$

The change in enthalpy upon mixing per unit volume, Δh_{mix}, is then readily obtained since

$$\Delta h_{mix} = \Delta g_{mix} + T\Delta s_{mix} = \Delta g_{mix} - T\left.\frac{\partial \Delta g_{mix}}{\partial T}\right|_{P,\phi_i} \quad (A2.5)$$

References and Notes

(1) Freeman, P. I.; Rowlinson, J. S. *Polymer* **1960**, *1*, 20.
(2) Bernstein, R. E.; Cruz, C. A.; Paul, D. R.; Barlow, J. W. *Macromolecules* **1977**, *10*, 681.
(3) Prigogine, I. *The Molecular Theory of Solutions*; North-Holland Publishing Co.: Amsterdam, 1959.
(4) Flory, P. J.; Orwoll, R. A.; Vrij, A. *J. Am. Chem. Soc.* **1964**, *86*, 3515.
(5) McMaster, L. P. *Macromolecules* **1973**, *6*, 760.
(6) Sanchez, I. C.; Lacombe, R. H. *Macromolecules* **1978**, *11*, 1145.
(7) Dudowicz, J.; Freed, K. F. *Macromolecules* **1991**, *24*, 5076; *Macromolecules* **1991**, *24*, 5096; *Macromolecules* **1991**, *24*, 5112.
(8) Hino, T.; Prausnitz, J. M. *Macromolecules* **1998**, *31*, 2636.
(9) Lipson, J. E. G. *Macromol. Theory Simul.* **1998**, *7*, 263.
(10) Luettmer-Strathmann, J.; Lipson, J. E. G. *Macromolecules* **1999**, *32*, 1093.
(11) Luettmer-Strathmann, J.; Lipson, J. E. G. *Phys. Rev. E* **1999**, *59*, 2039.
(12) Yeung, C.; Desai, R. C.; Shi, A.-C.; Noolandi, J. *Phys. Rev. Lett.* **1994**, *72*, 1834.
(13) Flory, P. J. *J. Chem. Phys* **1941**, *9*, 660.
(14) Flory, P. J. *Principles of Polymer Chemistry*; Cornell University Press: Ithaca, NY, 1953.
(15) Huggins, M. L. *J. Chem. Phys.* **1941**, *9*, 440.
(16) Huggins, M. L. *J. Chem. Phys.* **1942**, *46*, 151.
(17) Hildebrand, J. H.; Scott, R. L. *The Solubility of Non-Electrolytes*, 3rd ed.; Van Nostrand-Reinhold: Princeton, NJ, 1950.
(18) Krishnamoorti, R.; Graessley, W. W.; Dee, G. T.; Walsh, D. J.; Fetters, L. J.; Lohse, D. J. *Macromolecules* **1996**, *29*, 367.
(19) van Krevelen, D. W.; Hoftyzer, P. J. *Properties of Polymers. Correlation with Chemical Structure*; Elsevier: New York, 1972.
(20) de Gennes, P. G. *Scaling Concepts in Polymer Physics*; Cornell University Press: Ithaca, NY, 1979.
(21) Russell, T. P.; Hjelm, R. P.; Seeger, P. A. *Macromolecules* **1990**, *23*, 890.
(22) Freed, K. F.; Dudowicz, J. *J. Chem. Phys.* **1992**, *97*, 2105.
(23) Freed, K. F.; Dudowicz, J. *Macromolecules* **1996**, *29*, 625.
(24) Funk, E. W.; Prauznitz, J. M. *Ind. Eng. Chem.* **1970**, *62*, 8.
(25) Lacombe, R. H.; Sanchez, I. C. *J. Phys. Chem.* **1976**, *80*, 2568.
(26) Sanchez, I. C.; Panayiotou, C. G. *Models for Thermodynamic and Phase Equilibria Calculations*; Marcel Dekker: New York, 1994; p 187.
(27) Hammouda, B.; Bauer, B. J. *Macromolecules* **1995**, *28*, 4505.
(28) Janssen, S.; Schawhn, D.; Mortensen, K.; Springer, T. *Macromolecules* **1993**, *26*, 5587.
(29) Pollard, M.; Russell, T. P.; Ruzette, A. V.; Mayes, A. M.; Gallot, Y. *Macromolecules* **1998**, *31*, 6493.
(30) Lefebvre, A. A.; Lee, J. H.; Balsara, N. P.; Hammouda, B.; Krishnamoorti, R.; Kumar, K. *Macromolecules*, in press.
(31) Beiner, M.; Fytas, G.; Meier, G.; Kumar, S. K. *Phys. Rev. Lett.* **1998**, *81*, 594.
(32) Rodgers, P. A. *J. Appl. Polym. Sci.* **1993**, *48*, 1061.
(33) Sanchez, I. C. *Encyclopedia of Physical Science and Technology*, 2nd ed.; Academic Press: New York, 1992; Vol. XIII, pp 153−170.
(34) Ruzette, A.-V. G.; Banerjee, P.; Mayes, A. M.; Russell, T. P. *J. Chem. Phys.*, in press.
(35) Hildebrand, J. H. *J. Chem. Phys.* **1947**, *15*, 225.
(36) Lupis, C. H. P. *Chemical Thermodynamics of Materials*; Prentice-Hall: Englewood Cliffs, NJ, 1983.
(37) Hadziioannou, G.; Stein, R. S. *Macromolecules* **1984**, *17*, 567.
(38) Nishi, T.; Kwei, T. K. *Polymer* **1975**, *16*, 285.
(39) Lu, F. J.; Benedetti, E.; Hsu, S. L. *Macromolecules* **1983**, *16*, 1525.
(40) Garcia, D. *J. Polym. Sci., Polym. Phys. Ed.* **1984**, *22*, 107.
(41) Shibayama, M.; Yang, H.; Stein, R.; Han, C. *Macromolecules* **1985**, *18*, 2179.
(42) Amelino, L.; Martuscelli, E.; Sellitti, C.; Silvestre, C. *Polymer* **1990**, *31*, 1051.
(43) Beaucage, G.; Stein, R. S.; Hashimoto, T.; Hasegawa, H. *Macromolecules* **1991**, *24*, 3443.
(44) Hashimoto, T.; Hasegawa, H.; Hashimoto, T.; Katayama, H.; Kamigaito, M.; Sawamoto, M. *Macromolecules* **1997**, *30*, 6819.
(45) Han, C. C.; Bauer, J. B.; Clark, J. C.; Muroga, Y.; Matsushita, Y.; Okada, M.; Tran-cong, Q.; Chang, T.; Sanchez, I. C. *Polymer* **1988**, *29*, 2001.
(46) Nishimoto, M.; Takami, T. A.; Tohara, A.; Kasahara, H. *Polymer* **1994**, *36*, 1441.
(47) Friedrich, C.; Schwarzwälder, C.; Riemann, R.-E. *Polymer* **1995**, *37*, 2499.
(48) Jang, F. H.; Woo, E. M. *Polymer* **1999**, *40*, 2231.
(49) Weeks, N. E.; Karasz, F. E.; MacKnight, W. J. *J. Appl. Phys.* **1977**, *48*, 4068.

(50) Feng, H.; Feng, Z.; Ruan, H.; Shen, L. *Macromolecules* **1992**, *25*, 5981.
(51) Zoller, P.; Hoehn, H. *J. Polym. Sci., Polym. Phys. Ed.* **1982**, *20*, 1385.
(52) Callaghna, T. A.; Paul, D. R. *Macromolecules* **1993**, *26*, 2439.
(53) Siol, W. *Makromol. Chem., Macromol. Symp.* **1991**, *44*, 47.
(54) Roe, R. J.; Zin, W. C. *Macromolecules* **1980**, *13*, 1221.
(55) Rudolf, B.; Cantow, H.-J. *Macromolecules* **1995**, *28*, 6586.
(56) Ruzette, A. V. G.; Banerjee, P.; Mayes, A. M.; Pollard, M.; Russell, T. P.; Jerome, R.; Slawecki, T.; Hjelm, R.; Thiyagarajan, P. *Macromolecules* **1998**, *31*, 8509.
(57) Cowie, J. M. G.; Ferguson, R.; Fernandez, M. D.; McEwen, I. J. *Macromolecules* **1992**, *25*, 3170.
(58) Hasegawa, H.; Sakamoto, N.; Takeno, H.; Jinnai, H.; Hashimoto, T.; Schwahn, D.; Frielinghaus, H.; Janssen, S.; Imai, M.; Mortensen, K. *J. Phys. Chem. Solids* **1999**, *60*, 1307.
(59) Krishnamoorti, R.; Graessley, W. W.; Balsara, N. P.; Lohse, D. J. *Macromolecules* **1994**, *27*, 3073.
(60) Balsara, N. P.; Fetters, L. J.; Hadjichristidis, N.; Lohse, D. J.; Han, C. C.; Graessley, W. W.; Krishnamoorti, R. *Macromolecules* **1992**, *25*, 6137.
(61) Walsh, D. J.; Graessley, W. W.; Datta, S.; Lohse, D. J.; Fetters, L. J. *Macromolecules* **1992**, *25*, 5236.
(62) Lohse, D. J.; Fetters, L. J.; Doyle, M. J.; Wang, H. C.; Kow, C. *Macromolecules* **1993**, *26*, 3444.
(63) Krishnamoorti, R.; Graessley, W. W.; Fetters, L. J.; Garner, R. T.; Lohse, D. J. *Macromolecules* **1995**, *28*, 1252.
(64) Graessley, W. W.; Krishnamoorti, R.; Reichart, G.; Balsara, N.; Fetters, L. J.; Lohse, D. J. *Macromolecules* **1995**, *28*, 1260.
(65) Reichart, G. C.; Graessley, W. W.; Register, R. A.; Krishnamoorti, R.; Lohse, D. J. *Macromolecules* **1997**, *30*, 3363.
(66) Alamo, R. G.; Graessley, W. W.; Krishnamoorti, R.; Lohse, D. J.; Londono, J. D.; Mandelkren, L.; Stehling, F. C.; Wignall, G. D. *Macromolecules* **1997**, *39*, 5561.
(67) Reichart, G. C.; Graessley, W. W.; Register, R. A.; Krishnamoorti, R.; Lohse, D. J. *Macromolecules* **1997**, *30*, 3036.
(68) Foreman, K. W.; Freed, K. F. *J. Chem. Phys.* **1997**, *106*, 7422.
(69) Fredrickson, G. H.; Liu, A.; Bates, F. S. *Macromolecules* **1994**, *27*, 2503.
(70) Yethiraj, A.; Curro, J. G.; Rajasekaran, J. J. *J. Chem. Phys.* **1995**, *103*, 2229.
(71) Muller, M. *Macromolecules* **1995**, *28*, 6556.
(72) Curro, J. G. *Macromolecules* **1994**, *27*, 4665.
(73) Schweizer, K. S. *Macromolecules* **1993**, *26*, 6050.
(74) Schweizer, K. S.; Singh, C. *Macromolecules* **1995**, *28*, 2063.
(75) Singh, C.; Schweizer, K. S. *Macromolecules* **1997**, *30*, 1490.
(76) Maranas, J. K.; Mondello, M.; Grest, G. S.; Kumar, S. K.; Debenedetti, P. G.; Graessley, W. W. *Macromolecules* **1998**, *31*, 6991.
(77) Maranas, J. K.; Mondello, M.; Grest, G. S.; Kumar, S. K.; Debenedetti, P. G.; Graessley, W. W. *Macromolecules* **1998**, *31*, 6998.
(78) Bates, F. S.; Rosedale, J. H.; Fredrickson, G. H. *J. Chem. Phys.* **1990**, *92*, 6255.
(79) Rosedale, J. H.; Bates, F. S. *Macromolecules* **1990**, *23*, 2329.
(80) Fowler, M. E.; Barlow, J. W.; Paul, D. R. *Polymer* **1987**, *28*, 1177.
(81) Nishimoto, M.; Keskkula, H.; Paul, D. R. *Macromolecules* **1990**, *23*, 3633.
(82) Hahn, K.; Schmitt, B. J.; Kirschey, M.; Kirste, R. G.; Salie, H.; Schimtt-Strecker, S. *Polymer* **1992**, *33*, 5150.
(83) Chiu, S.-C.; Smith, T. G. *J. Appl. Polym. Sci.* **1984**, *29*, 1797.
(84) Svoboda, P.; Kressler, J.; Ougizawa, T.; Inoue, T. *Macromolecules* **1997**, *30*, 1973.
(85) Callaghan, T. A.; Takakuwa, K.; Paul, D. R. *Polymer* **1993**, *34*, 3797.
(86) Li, H.; Yang, Y.; Fujitsuka, R.; Ougizawa, T.; Inoue, T. *Polymer* **1999**, *40*, 927.
(87) Kim, W. N.; Burns, C. *Macromolecules* **1987**, *20*, 1876.
(88) Nishimoto, M.; Paul, D. R. *Polymer* **1991**, *32*, 1274.
(89) Callaghan, T. A.; Paul, D. R. *J. Polym. Sci., Polym. Phys. Ed.* **1994**, *32*, 1813.
(90) Hopkinson, I.; Kiff, F. T.; Richards, R. W.; King, S. M.; Farren, T. *Polymer* **1995**, *36*, 3523.
(91) Ito, H.; Russell, T. P.; Wignall, G. D. *Macromolecules* **1987**, *20*, 2213.
(92) Walsh, D. J.; McKeown, G. J. *Polymer* **1980**, *21*, 1331.
(93) Walsh, D. J.; Cheng, G. L. *Polymer* **1984**, *25*, 495.
(94) Tremblay, C.; Prud'Homme, R. E. *J. Polym. Sci., Polym. Phys. Ed.* **1984**, *22*, 1857.
(95) Benedetti, E.; Catanorchi, S.; D'Alessio, A.; Vergamini, P.; Ciardelli, F.; Pracella, M. *Polym. Int.* **1998**, *45*, 373.
(96) Choi, K.; Jo, W. H.; Hsu, S. L. *Macromolecules* **1998**, *31*, 1366.
(97) Yi, Y. X.; Zoller, P. *J. Polym. Sci., Part B: Polym. Phys.* **1993**, *31*, 779.
(98) Han, S. J.; Lohse, D. J.; Condo, P. D.; Sperling, L. H. *J. Polym. Sci., Part B: Polym. Phys.* **1999**, *37*, 2835.
(99) Leibler, L. *Macromolecules* **1980**, *13*, 1602.
(100) Isrealachvili, J. *Intermolecular and Surface Forces*; Academic Press: San Diego, 1991; pp 18−19.

MA000712+